Heterogeneity of morphometric similarity networks in health and schizophrenia

Joost Janssen[1,2,±,*], Ana Guil Gallego[1,*], Covadonga M. Díaz-Caneja[1,2,3], Noemi González Lois[1], Niels Janssen[4,5,6], Javier González-Peñas[1,2], Pedro M. Gordaliza[7,8], Elizabeth E.L. Buimer[9], Neeltje E.M. van Haren[9,10], Celso Arango[1,2,3], René S. Kahn[9,11], Hilleke E. Hulshoff Pol[9] & Hugo G. Schnack[9,10,12]

[1]Department of Child and Adolescent Psychiatry, Institute of Psychiatry and Mental Health, Hospital General Universitario Gregorio Marañón, Instituto de Investigación Sanitaria Gregorio Marañón (IiSGM), Madrid, Spain.
[2]Ciber del Área de Salud Mental (CIBERSAM), Instituto de Salud Carlos III, Madrid, Spain.
[3]School of Medicine, Universidad Complutense, Madrid, Spain.
[4]Department of Psychology, Universidad de la Laguna, Tenerife, Spain.
[5]Institute of Biomedical Technologies, Universidad de La Laguna, Tenerife, Spain.
[6]Institute of Neurosciences, Universidad de la Laguna, Santa Cruz de Tenerife, Spain.
[7]CIBM Center for Biomedical Imaging, Lausanne, Switzerland
[8]Radiology Department, Lausanne University Hospital (CHUV) and University of Lausanne, Lausanne, Switzerland
[9]Department of Psychiatry, UMCU Brain Center, University Medical Center Utrecht, Utrecht, The Netherlands.
[10]Department of Child and Adolescent Psychiatry/Psychology, Erasmus University Medical Centre, Sophia Children's Hospital, Rotterdam, The Netherlands.
[11]Department of Psychiatry, Icahn School of Medicine at Mount Sinai, New York, United States.
[12]Department of Languages, Literature, and Communication, Faculty of Humanities, Utrecht University, Utrecht, The Netherlands
±Corresponding author
*Contributed equally
Word count abstract:
Word count text body:
Short title:
Figures: Embedded in text body
Tables:

Correspondence to:
Joost Janssen, PhD
Department of Child and Adolescent Psychiatry
Hospital General Universitario Gregorio Marañón
C/ Ibiza, 43. 28009-Madrid, Spain
Phone: 0034914265005
Fax: 0034914265004
Mail: joost.janssen76@gmail.com

Abstract

Introduction

Morphometric similarity is a recently developed neuroimaging phenotype of inter-regional connectivity by quantifying the similarity of a region to other regions based on multiple MRI parameters. Altered average morphometric similarity has been reported in psychotic disorders at the group level, with considerable heterogeneity across individuals. We used normative modeling to address cross-sectional and longitudinal inter-individual heterogeneity of morphometric similarity in health and schizophrenia.

Methods

Morphometric similarity for 62 cortical regions was obtained from baseline and follow-up T1-weighted scans of healthy individuals and patients with chronic schizophrenia. Cortical regions were classified into seven predefined brain functional networks. Using Bayesian Linear Regression and taking into account age, sex, image quality and scanner, we trained and validated normative models in healthy controls from eleven datasets (n = 4310). Individual deviations from the norm (z-scores) in morphometric similarity were computed for each participant for each network and region at both timepoints. A z-score $\geqq$ than 1.96 was considered supra-normal and a z-score $\leqq$ -1.96 infra-normal. As a longitudinal metric, we calculated the change over time of the total number of infra- or supra-normal regions per participant.

Results

At baseline, patients with schizophrenia had decreased morphometric similarity of the default mode network and increased morphometric similarity of the somatomotor

network when compared with healthy controls. The percentage of patients with infra- or supra-normal values for any region at baseline and follow-up was low (<6%) and did not differ from healthy controls. Mean intra-group changes over time in the total number of infra- or supra-normal regions were small in schizophrenia and healthy control groups (<1) and there were no significant between-group differences.

Conclusions

In a case-control setting, a decrease of morphometric similarity within the default mode network may be a robust finding implicated in schizophrenia. However, normative modeling suggests that significant reductions and changes over time of regional morphometric similarity are evident only in a minority of patients.

Introduction

Schizophrenia is a severe psychiatric disorder that affects about 1% of the global population (Jauhar et al., 2022). Despite decades of research, the prognosis in a substantial proportion of patients remains poor (Jauhar et al., 2022). A considerable challenge hindering the development of more effective, personalized treatment strategies for schizophrenia lies in the unresolved neurobiological heterogeneity that characterizes the disease (Alnæs et al., 2019; Brugger and Howes, 2017). While morphological reductions in brain volume and cortical thickness may be relatively robust at the group level in schizophrenia, there is considerable variation across individuals (Brugger and Howes, 2017; Haijma et al., 2013; Kelly et al., 2018; Segal et al., 2023; van Erp et al., 2018). The normative modeling framework aims to address the issue of individual phenotypic heterogeneity by establishing normative standards for neurobiological variables and subsequently assessing individual's deviation from these norms (Marquand et al., 2019). Studies applying normative model analysis in schizophrenia are relatively sparse but have shown that abnormal deviations of regional cortical thickness and volume are frequent at the individual level but rarely occur consistently in the same locations and with the same severity across individuals (Di Biase et al., 2022; Lv et al., 2021; Segal et al., 2023; Wolfers et al., 2018).

Morphometric similarity is a recently developed neuroimaging phenotype of cortical inter-regional connectivity by quantifying the similarity of a region to all other regions based on multiple MRI parameters assessed at each region (Sebenius et al., 2023; Seidlitz et al., 2018). That is, each brain region is represented as a vector of several MRI features, such as cortical thickness and volume, and based on the

pairwise correlation between the regional feature vectors, morphometric similarity can be estimated.

Morphometric similarity has been validated as a proxy for inter-regional connectivity, as regions with high morphometric similarity show stronger axonal connectivity (Seidlitz et al., 2018). In contrast to cortical volume and thickness, little is known about the typical age-dependency of morphometric similarity between late childhood and old age. Normative modeling in a large sample of healthy controls with a wide age range provides an excellent opportunity to characterize regional differences in the age-dependency of typical morphometric similarity (Zhukovsky et al., 2022). In psychosis, morphometric similarity has shown recent promise as a relevant phenotype because findings of reduced average morphometric similarity in frontal and temporal regions have been replicated in three independent groups of adult individuals with psychosis and one group of individuals with early-onset schizophrenia (Morgan et al., 2019; Yao et al., 2023). In addition, a disproportionate number of regions that showed group-average reductions in morphometric similarity in individuals with psychosis were part of the default mode network (DMN) which concurs with DMN deficits reported from functional MRI studies (Broyd et al., 2009; Heuvel and Sporns, 2019; Morgan et al., 2019). However, it is worth noting that diagnostic investigations into morphometric similarity have predominantly relied on cross-sectional group-level averages, thereby overlooking potentially substantial heterogeneity of morphometric similarity at the individual level (Morgan et al., 2019; Yao et al., 2023; Zhukovsky et al., 2022).

Longitudinal assessments of morphometric similarity combined with normative modeling allows not only for cross-sectional quantification of individual deviation but also enables assessment of intra-individual change in deviation over time and its

relation to the established normative range (Barbora Rehák Bučková et al., 2024; Di Biase et al., 2023).

Here, we apply a normative modeling framework to morphometric similarity and conduct a longitudinal study of this metric for the first time. In this study, we aim to parse the cross-sectional and longitudinal heterogeneity of morphometric similarity in schizophrenia, by assessing a longitudinal sample of adult individuals with schizophrenia and healthy controls.

Methods

Sample

Eleven datasets were combined to create the full sample. These datasets are described in Figure A including the sample size, age, and sex distribution of each dataset. We included healthy participants from ten publicly available datasets: the Amsterdam Open MRI Collection (aomic) (id1000, piop1 and piop2) datasets (Snoek et al., 2021), the Cambridge Centre for Ageing and Neuroscience (camcan) dataset (Shafto et al., 2014), the Dallas Longitudinal Brain Study (dlbs) dataset (Lu et al., 2011), the Information eXtraction from Images (ixi) dataset (http://brain-development.org/ixidataset/), the Narratives (narratives) dataset (Nastase et al., 2021), the Open Access Series of Imaging Studies (oasis3) dataset (Marcus et al., 2010), the NKI-Rockland (rockland) dataset (Nooner et al., 2012) and the Southwest University adult lifespan (sald) dataset (Wei et al., 2018). One dataset is not publicly available and consisted of a large longitudinal sample of individuals with schizophrenia and healthy participants aged 16-68 years (at baseline) from the Utrecht Schizophrenia project and the Genetic Risk and Outcome of Psychosis (GROUP) consortium. From this longitudinal clinical sample we included individuals who had T1-weighted magnetic resonance imaging (MRI) scan acquisitions at baseline and follow-up. Two identical scanners were used and all included participants had their baseline and follow-up scans acquired on the same scanner. Detailed information regarding diagnostic criteria, clinical assessments, MRI acquisition and image quality control assessment of the Utrecht Schizophrenia project and the GROUP consortium are described in (Hulshoff Pol et al., 2001; Janssen et al., 2021; Korver et al., 2012; Kubota et al., 2015). Additional demographic, cognitive, and clinical characteristics of the longitudinal clinical sample

6

are provided in Table A. All participants provided written informed consent. Subject recruitment procedures and informed consent forms, including consent to share de-identified data, were approved by the corresponding institutional review board where data were collected.

Site	N (subjects)	Age (mean years (SD))	Sex (%F)
aomic_id1000	927	22.85 (1.71)	52.1
aomic_piop1	209	22.18 (1.80)	57.4
aomic_piop2	224	21.96 (1.79)	57.1
camcan	645	54.53 (18.48)	50.9
dlbs	309	54.09 (19.91)	62.1
ixi	456	50.82 (16.15)	56.1
narratives	336	21.92 (4.66)	58.9
oasis3	615	69.44 (8.75)	59.7
rockland	495	39.70 (22.96)	66.1
sald	494	45.18 (17.44)	62.1
clinical_baseline	459	30.24 (10.43)	36.6
clinical_follow_up	459	34.25 (10.71)	36.6

Figure A. Eleven datasets were used in the study. Ten datasets were cross-sectional and included healthy participants. For each of these ten datasets, 90% of individuals were included in the training set and 10% were part of the test set. One longitudinal clinical dataset (two timepoints) included healthy controls and individuals with chronic schizophrenia. Of the healthy controls belonging to the longitudinal clinical dataset, 20% were included in the training set and 80% in the test set. All individuals with schizophrenia were included in the test set. The age distribution for each dataset within the training/test samples is shown. The table shows the descriptives per dataset. N, number of subjects.

	Healthy		Schizophrenia	
	Baseline (N=292)	Follow-up (N=292)	Baseline (N=167)	Follow-up (N=167)
Age (years)	30.44 (11.02)	34.39 (11.31)	29.90 (9.31)	34.02 (9.60)
Sex (N, (%F))	130 (44.5)		38 (22.8)	
Education (years)	21.92 (25.33)		20.31 (25.84)	
IQ total	110.28 (15.79)	113.89 (16.65)	97.82 (16.60)	103.13 (20.34)
Time between scans (years)	3.95 (1.03)		4.11 (0.95)	
Age of onset (years)			22.14 (5.28)	
Illness duration at scan (years)			6.41 (6.66)	11.08 (7.72)
PANSS total			63.22 (19.38)	50.17 (14.28)
Total Positive			14.91 (5.85)	12.38 (4.65)
Total Negative			16.25 (6.25)	12.83 (5.66)
Total General			31.15 (11.26)	24.97 (7.04)

Table A. Demographic, cognitive, imaging, and clinical characteristics of the clinical dataset. All descriptors are mean (standard deviation) unless otherwise specified. N, number of subjects; F, female; PANSS, Positive and Negative Syndrome Scale (Kay et al., 1987).

Image processing and quality control

All T1-weighted images from all datasets were processed centrally using the FreeSurfer analysis suite (v7.1) with default settings (Fischl, 2012). Estimates of 1) cortical volume, 2) surface area, 3) average cortical thickness, 4) average curvature, and 5) Gaussian curvature were calculated for each of the 62 regions of the

8

Desikan-Killany-Tourneville (DKT) atlas (Klein and Tourville, 2012). The Freesurfer Euler number was extracted as a proxy for image quality (Rosen et al., 2018). Subjects were removed if the maximum, absolute, within-dataset centered Euler number was larger than 10 (Rutherford et al., 2023).

Morphometric similarity

Using regional measurements of cortical thickness, surface area, cortical volume, mean curvature and Gaussian curvature we calculated regional morphometric similarity following a previously published protocol (Seidlitz et al., 2018), see Figure B-A and B-B. We assessed the replicability of our approach by comparing regional morphometric similarity maps to previously published maps (Morgan et al., 2019). The correlation between our regional morphometric similarity maps and the previously published maps by Morgan et al. (2019) was 0.8, thus indicating good replicability; see the Supplemental text and Supplemental Figure A for details.

Mapping the DKT atlas regions to functional networks

We focused on seven widely recognized functional brain networks derived from an analysis of an independent resting state fMRI dataset (Thomas Yeo et al., 2011), see Supplemental Figure B. To obtain a correspondence between the regions of the DKT atlas and the seven functional networks we followed the approach by (Váša et al., 2018). Briefly, for each region of the DKT atlas we calculated the overlap (as the number of vertices) between each region of the DKT atlas and with each of the seven functional networks. Thereafter, for each region, the largest

overlap determined to which functional network an region was ascribed. This resulted in a mapping of each region to one of the seven functional networks.

Normative modeling of morphometric similarity

For normative modeling, each of the ten datasets containing only healthy controls was split into a training set (90%) and a test set (10%), see Figure A. For the clinical dataset, all individuals with schizophrenia as well as 80% of the healthy controls were included in the test set while the remaining healthy controls (20%) were included in the training set. The per-dataset splits were created using the createDataPartition function from the caret R package, preserving the distribution of age, sex, and scanner (some datasets contained multiple scanners) in both the training and the test split of each dataset. The training set included 4,310 participants and the test set 859 participants. Bayesian Linear Regression (BLR) with likelihood warping using a B-spline (spline order=3, number of knots=5) was used to predict morphometric similarity from a vector of covariates (age, sex, Euler number, and scanner) (Rutherford et al., 2023). For a complete mathematical description and explanation of this implementation, see (Fraza et al., 2021). Briefly, for each brain region of interest (r),

$$y_r = w^T \phi(X) + \epsilon_s \qquad (1)$$

where y is the predicted distribution of morphometric similarity for region r, w^T is the estimated weights vector, X is the set of covariates, $\phi(X)$ the B-spline basis expansion applied to them, and ϵ_s a gaussian noise distribution term for scanner *s*.

Individual deviations: infra- and supra-normal morphometric similarity

10

Our normative model is cross-sectional. We followed the method proposed by Barbora Rehák Bučková et al (2024) who showed that longitudinal normative modeling metrics (see Statistics) for adult individuals with schizophrenia and healthy participants can be calculated from a large cross-sectional normative model of healthy participants (Barbora Rehák Bučková et al., 2024). We created morphometric similarity normative charts for each region using the training set consisting of healthy participants. Thereafter, individuals from the test set were positioned on the morphometric similarity normative charts. For each individual deviation (z) scores, quantifying individual deviation from the normative average, were calculated for all brain regions (r) and all participants (n), as follows:

$$z_{nr} = \frac{y_{nr} - \widehat{y_{nr}}}{\sqrt{\sigma_r^2 + (\sigma_*^2)_r}}$$ (2)

where y_{nr} means the true morphometric similarity value and $\widehat{y}_{nr}$ is the predicted mean morphometric similarity value. The difference in these values is normalized to account for two different sources of variation; i) σ_r^2, which is the aleatoric uncertainty and reflects the variation between individuals across the population, and ii) the epistemic uncertainty, σ_{*r}^2, which accounts for the variance associated to modeling uncertainty introduced by the model assumptions or parameter selection. Z-scores were then categorized as either: (i) normal, i.e. within the normative range of variation for healthy individuals with the same age range, sex, Euler number, and scanner; (ii) supra-normal: significantly exceeding the normative range; or, (iii) infra-normal: significantly below the normative range. As per previous studies (Bethlehem et al., 2020; Di Biase et al., 2022; ENIGMA Clinical High Risk for Psychosis Working Group et al., 2024; Huang et al., 2024; Janssen et al., 2021; Lv

11

et al., 2021; Rutherford et al., 2023) we considered a z-score $\geqq$ than 1.96 as supra-normal and a z-score $\leqq$ -1.96 as infra-normal.

Evaluation of the normative model

The unseen data in the complete test set was used to evaluate the normative model. The evaluation included Q-Q plots, and the metrics proportion of explained variance, mean standardized log loss, standardized mean square error, root mean square error, rho, bayesian information criterion, skewness, and kurtosis (see Supplemental Figure C).

Statistical analyses

The typical age-dependency of regional morphometric similarity

Normative modeling allowed us to assess the age-dependency of normative morphometric similarity across cortical regions from late childhood to old age. We tested whether the regions could be clustered into distinct groups of regions based on the shape of the age-dependence of MS, see Figure B-D. We therefore binned the training set along the age range into 27 equally-sized age bins (3.6 years/bin). Thereafter, a 62x27 matrix was constructed where each row was a region and each column contained the median normative morphometric similarity (50th percentile) of a particular age bin. Principal Component Analysis was applied to the matrix using the prcomp R package. The resulting Euclidean distance matrix was used for hierarchical clustering. The optimal number of clusters was determined using the NbClust R package, which generates 23 cluster solutions using different methods and from which the optimal number of clusters is chosen by majority voting (Charrad et al., 2014).

Effects of diagnosis on morphometric similarity of functional networks

Averaged z-scores of the seven functional networks were compared between healthy controls and individuals with schizophrenia at baseline using Welch t-tests. Effect sizes are given as Cohen's d. Only p values that survived FDR correction for multiple comparisons were considered significant.

The percentage of individuals with infra- or supra-normal deviance per region

We calculated for each region (r) and at each timepoint (*t* = *t*1 or *t*2) the percentage of patients and healthy controls that had supra- or infra-normal z-scores:

$$percentage\ outliers_r(t) = \frac{\sum_{n=1}^{N_{total}} \delta_{rn}(t)}{N_{total_t}} \cdot 100\% \tag{3}$$

where $\delta_{rn}(t)$ equals 1 if participant *n*=1,...,N_{total} has |Z| > 1.96 in region r at time point *t*, and equals 0 otherwise and N_{total} is the total number of participants at time point *t*. Group differences for each region and at each time point in the proportion of individuals with supra- or infra-normal z-scores were examined using the two-proportions z-test.

Differences in percentage of outliers over time by region are calculated by subtracting the baseline percentage from the follow-up percentage for each region r:

$$change\ in\ outlier\ percentage_r(t) = percentage\ outliers_r(t2) - percentage\ outliers_r(t1) \tag{4}$$

To assess the spatial distribution of infra- and supra-normal deviations we built diagnostic-wise brain maps, see Figure B-E.

Effects of diagnosis on the amount of outlier regions per participant

Here we determine the change over time in total number of outlier regions per participant as follows:

$$change\ in\ outlier\ count_n(t) = \sum_{r=1}^{62} \delta_{rn}(t1) - \sum_{r=1}^{62} \delta_{rn}(t2) \tag{5}$$

where δ equals 1 if participant n has $|Z| > 1.96$ for region r=1,...,62, and equals 0 otherwise. Diagnostic group differences in the change in total number of outlier regions by participant were examined using a Welch t-test. In the group of individuals with schizophrenia we tested for associations between change in outlier count over time and IQ and PANSS positive, negative and general scores using Pearson correlation.

Supplemental analyses

Firstly, we repeated the analysis of clustering of regions based on normative models for males and females separately to assess whether results differed by sex. Secondly, we calculated infra- and supra-normal deviance for males and females separately to assess whether results differed by sex. Thirdly, we assessed whether using z-scores from normative modeling led to stronger diagnostic group results as compared to using 'raw' morphometric similarity (i.e., the traditional approach). Fourthly, we averaged morphometric similarity across all regions and hemispheres to determine whole brain morphometric similarity and compared this between cases and controls.

14

Results

Visualization and evaluation of the normative models

An exemplary normative model plot with percentile curves for the left hemispheric superior frontal gyrus can be seen in Figure B-C. Distributions of the evaluation metrics of the normative models can be found in Supplemental Figure C.
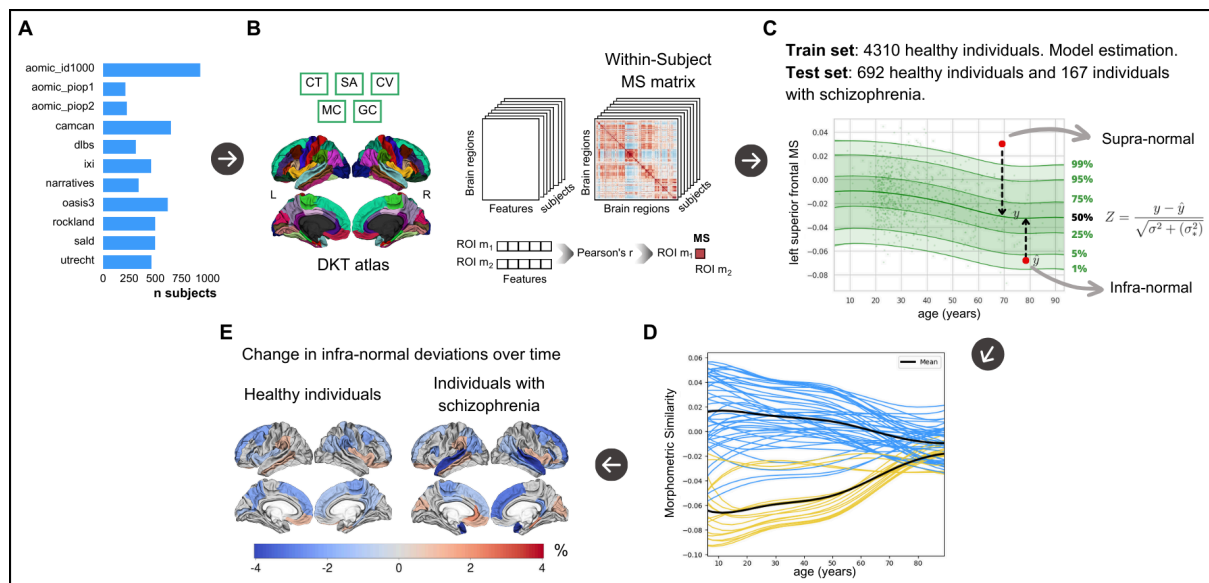

Figure B. Study overview. **A**. Ten cross-sectional datasets consisting of healthy individuals only and one longitudinal dataset consisting of healthy controls and individuals with chronic schizophrenia (utrecht) were used in the study. **B**. morphometric similarity matrices were constructed following established protocols using cortical thickness, cortical volume, surface area, mean curvature and Guassian curvature extracted for each cortical region (Seidlitz et al., 2018). **C**. Example centile plot from normative modeling of regional morphometric similarity of the left hemispheric superior frontal gyrus for assessing individual deviance (Z). Normative modeling was done following established protocols (Rutherford et al., 2022) using prediction on unseen test data following training of the model. **D**. Normative models of each cortical region were clustered based on their typical age-dependency. **E**.

Cortical maps depicting percentage longitudinal change of extreme deviance below the norm, i.e. infra-normal deviance, in individuals with schizophrenia and healthy individuals. n, number of subjects, CT, cortical thickness; SA, surface area; CV, cortical volume; MC, mean curvature; GC, Gaussian curvature. MS, morphometric similarity.

The typical age-dependency of regional morphometric similarity

Principal component analysis using the age-dependency of regional morphometric similarity revealed that the first two principal components explained 98.63% of the variance (first component: R^2=77.14%, second component: R^2=21.49%) of the median normative morphometric similarity across age groups and were therefore selected for constructing the distance matrix, see Figure C. Clustering gave two clusters as the optimal solution. As can be seen in Figure C, clustering was extremely similar between left and right hemispheres. The first cluster (number of regions = 44, 71% of all regions) includes mostly frontal and temporal regions with positive morphometric similarity tending towards zero during aging. The second cluster (18 regions, 29%) consists of inferior prefrontal, postcentral gyrus and occipital regions with negative morphometric similarity tending towards zero during aging.

39% of all regions from Cluster 1 were part of the default mode network which is significantly more than expected (P<0.001, one sample z-test for proportions, see Table B). For Cluster 2 this was 11% (P=0.48).
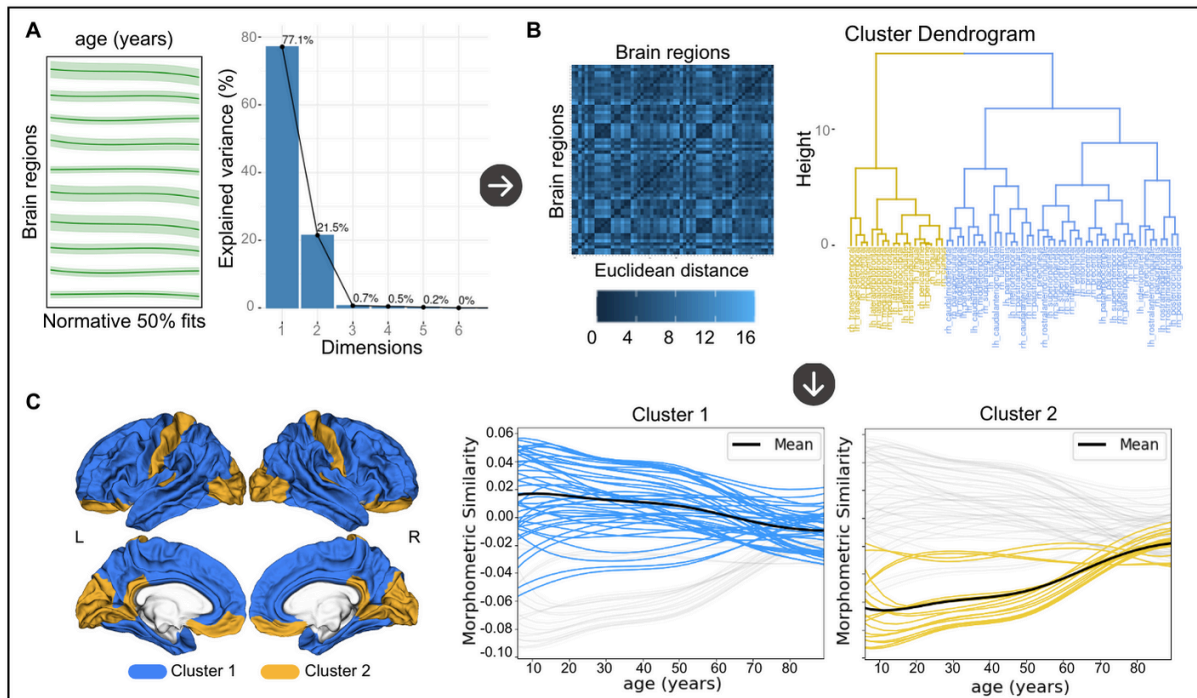
Figure C. Clustering of brain regions based on the typical age-dependency of regional morphometric similarity. **A**. The median normative morphometric similarity of the normative model of each cortical region was entered into a Principal Component Analysis (PCA). The first two components explaining 98.6% of the variance were selected. **B**. The Euclidean distance matrix was extracted from the PCA output and used for hierarchical clustering. A two cluster solution was determined optimal. **C**. Each plot shows the median normative fits for a cluster with the remaining normative fits in gray. The average fit across all fits belonging to a cluster is added in black. The cluster solution was also visualized on the cortex displaying the distribution of the two clusters across the cortex. L, left hemisphere, R, right hemisphere. The upper row are lateral views, the bottom row are medial views.

Network	MS Cluster 1	MS Cluster 2
Visual	2	6
Somato Motor	2	2
Dorsal Attention	4	4
Ventral Attention	8	0
Limbic	9	0
Fronto Parietal	2	4
Default Mode	17	2

Table B. Number of regions from each of the two clusters belonging to each of the seven functional networks. MS, morphometric similarity.

Effects of diagnosis on morphometric similarity of functional networks

At baseline, the group of individuals with schizophrenia had a positive average deviance of morphometric similarity for the somatosensory network which differed significantly from the negative average deviance of morphometric similarity in healthy controls (d=0.30; p<0.01). Individuals with schizophrenia had a negative average deviance of morphometric similarity for the default mode network which differed significantly from the positive average deviance of morphometric similarity in healthy controls (d=-0.36; p<0.001), see Table C and Figure D. At follow-up, the group of individuals with schizophrenia maintained the negative morphometric similarity for the default mode network compared to healthy controls but this difference did not withstand correction for multiple comparisons, see Figure D.

18

Timepoint	Network	z-scores	
		t-statistic	$P\ value^{A}$
Baseline	Visual	1.451	0.148
	Somato Motor	2.940	0.003*
	Dorsal Attention	-0.844	0.399
	Ventral Attention	-0.075	0.940
	Limbic	-1.902	0.058
	Fronto Parietal	-0.805	0.421
	Default Mode	-3.665	0.0002*
Follow-up	Visual	1.519	0.130
	Somato Motor	1.675	0.095
	Dorsal Attention	-0.867	0.387
	Ventral Attention	-0.819	0.413
	Limbic	-0.617	0.537
	Fronto Parietal	-0.361	0.718
	Default Mode	-2.046	0.041

Table C. Results of statistical tests for case-control differences in z-scores averaged across regions belonging to the seven functional brain networks (Thomas Yeo et al., 2011). A positive t-statistic indicates that the group of individuals with schizophrenia has a higher mean than the group of healthy controls, while a negative t-statistic

indicates that the group of individuals with schizophrenia has a lower mean MS than the group of healthy controls. *$P_{FDR} < 0.05$.
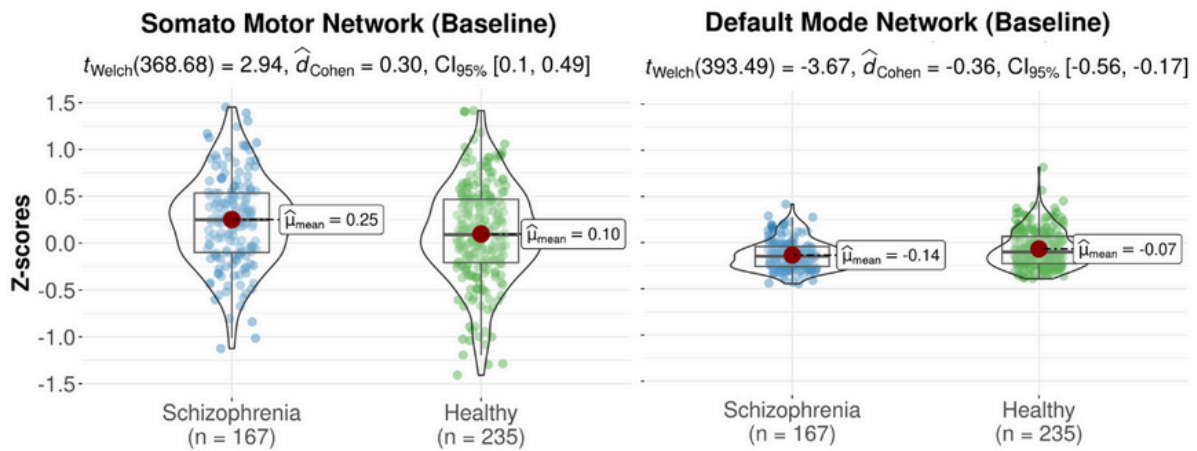

Figure D. Violin plots of significant (FDR-corrected) differences in z-scores of morphometric similarity of two functional networks that differed significantly between the group of healthy controls and the group of individuals with schizophrenia at baseline.

The percentage of individuals with infra- or supra-normal deviance per region

The percentage of individuals from the test set with either infra- or supra-normal deviance was below 6% for both the healthy individual and the schizophrenia samples at the baseline and follow-up visits (see Figure E-A and E-B). At both timepoints, the percentage of infra-normal regional morphometric similarity z-scores ranged between 0 and 6.0% for individuals with schizophrenia and between 0 and 4.3% for healthy individuals; for supra-normal morphometric similarity z-scores percentage ranges were 0–5.4% and 0–6.0%, respectively. There were no significant differences between patients and controls in the percentage of participants with infra- or supra-normal regional values at either baseline or follow-up (P>0.05). At baseline and follow-up, the percentages of individuals with schizophrenia with infra-normal

deviance were highest in the superior temporal and superior frontal regions. For both diagnostic groups, the percentages of participants with supra-normal deviance were highest in the occipital lobe and postcentral gyrus (see Figure E-A and E-B).

We then assessed differences in longitudinal change in the percentage of outlier individuals for each region between cases and controls, separately for infra- and supra-normal deviance. For a majority of regions, and both for cases and controls, the change in percentage of outliers with infra-normal deviance was negative while this was not the case for the change in percentage of supra-normal deviance (see Figure E-C). This indicated that for the majority of regions, 'normalizing' of outlier participants over time occurred more frequently in regions where those outliers initially had infra-normal deviance compared to regions where those outliers initially had supra-normal deviance. For infra-normal deviance the regions with highest percentages of change were the bilateral superior temporal and left superior and medial frontal regions with a decrease over time of 4.2%, 0.6% and 1.8%, respectively. For supra-normal deviance the region with the highest percentage of change was the left postcentral gyrus with an increase of 1.2% (see Figure E-C).
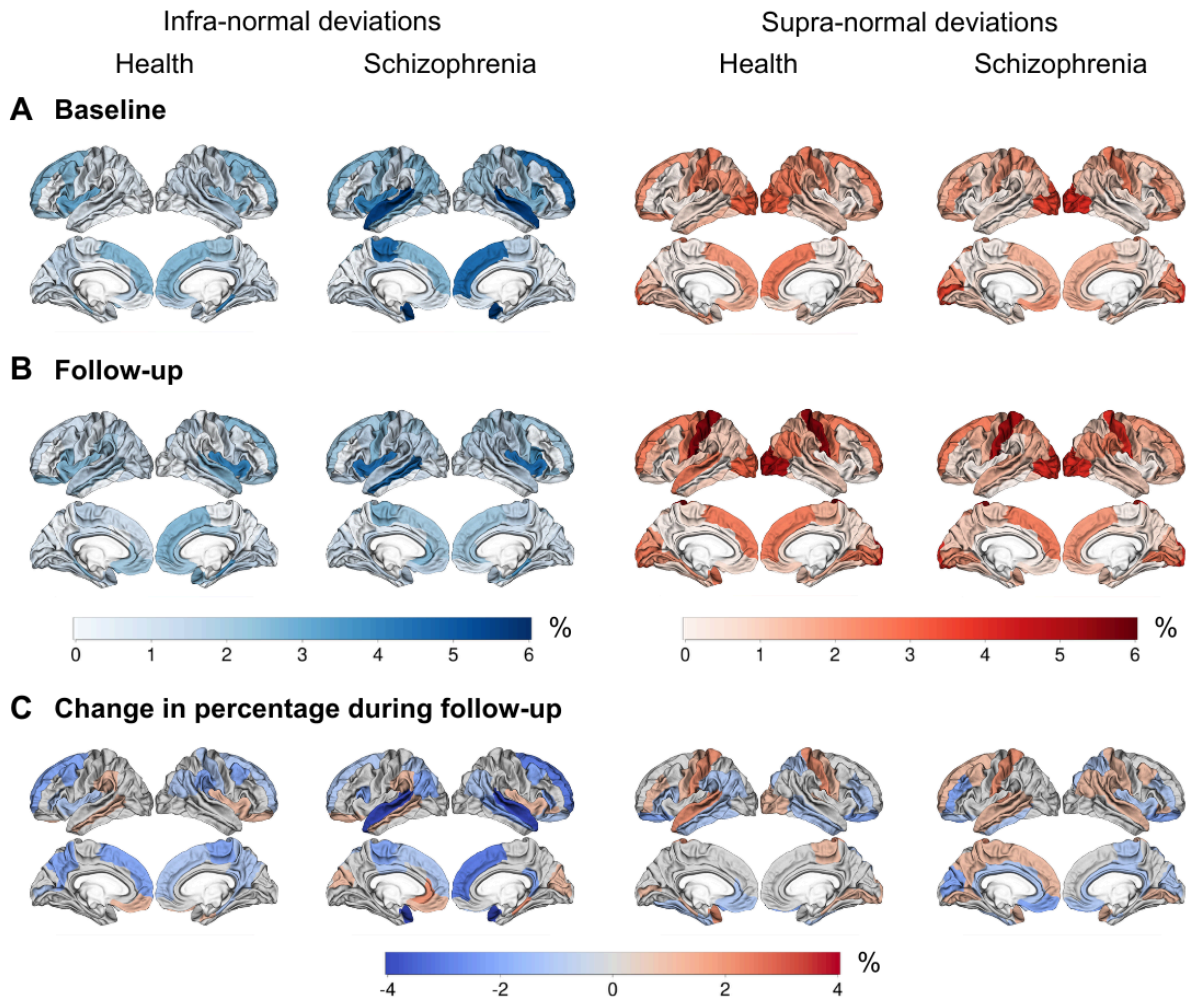
Figure E. Cortical maps showing the percentage of individuals with infra- and supra-deviance morphometric similarity per region, **A**) at baseline, **B**) at follow-up, and **C**) the change in percentage during follow-up (i.e., percentage at follow-up - percentage at baseline). A negative percentage means that the regional percentage of individuals with infra- or supra-normal deviance decreased during follow-up.

Effects of diagnosis on the amount of outlier regions per participant

No significant group differences for the average cross-sectional total outlier count and change in total outlier region count over time were found between healthy controls and individuals with schizophrenia (see Supplemental Figure D).

In the group of individuals with schizophrenia no significant correlations were found between cross-sectional outlier region count or change in outlier region count over time and IQ and PANSS scores (P>0.05).

Supplemental analyses

Clustering of regions based on normative models showed three clusters in males and two clusters in females as the optimal solution (see Supplemental Figure E).

Across both time points and regions, the percentage of female participants with either infra- or supra-normal deviance at baseline and follow-up was higher compared to males. In both sexes there were no significant differences in the percentage of individuals with infra- or supra-normal regional values at baseline and follow-up (see Supplemental Text and Supplemental Figures F and G).

We replicated the finding of lower average deviance morphometric similarity for the default mode network for the group of individuals with schizophrenia compared to healthy controls in the analyses using raw values at baseline, albeit with a smaller effect size (d=-0.27, p<0.01) compared to the normative-modeling based z-scores (see Supplemental Table A, Supplemental Text and Supplemental Figure H).

There was no difference of whole brain morphometric similarity between individuals with schizophrenia and healthy individuals (see Supplemental Figure I).

Discussion

To the best of our knowledge this study is the first longitudinal study of morphometric similarity, as well as the first to assess morphometric similarity in a normative modeling framework. We established regional age-dependent normative trajectories for morphometric similarity across the adult age range. We found that, overall,mean regional morphometric similarity converged towards zero with increasing age, which is coherent with a prior study (Zhukovsky et al., 2022). Here, we extended prior findings by showing that age-dependent trajectories can be clustered into two groups. One cluster contains trajectories that start with positive morphometric similarity values at younger ages which decrease to zero with age. The other cluster starts with negative morphometric similarity values which increase to zero with age. We also showed that the default mode network contained disproportionally more regions of the former compared to the latter cluster. Studies have consistently reported age-related reductions in resting-state functional connectivity of the default mode network as well as structural network connectivity (Cox et al., 2016; Geerligs et al., 2015). As such, these findings are in line with the observed decline of morphometric similarity across a large age range. In addition, this finding provides support for the notion that brain structure, at least partially, underlies function (Pang et al., 2023; Zhukovsky et al., 2022).

Our investigation aimed to compare morphometric similarity across functional networks and regions between individuals with schizophrenia and healthy subjects over time.

Our cross-sectional findings revealed that, at baseline, individuals diagnosed with schizophrenia exhibited increased morphometric similarity across regions pertaining to the somato-motor network and decreased morphometric similarity

24

across regions pertaining to the default mode network when compared to the healthy control subjects. The reduced morphometric similarity in the group of individuals with chronic schizophrenia aligns with previous research morphometric similarity findings as well as general default mode dysfunction in high-risk, early-onset and chronic schizophrenia (Morgan et al., 2019; Whitfield-Gabrieli et al., 2009; Yao et al., 2023). A recent study demonstrated that morphometric similarity was positively correlated with the likelihood of cellular network structures forming axonal connections (Lin et al., 2024). In schizophrenia, axonal dysconnectivity between networks might lead to the micro-structural and functional connectivity deficits observed across various age groups affected by the disease, including children, adolescents, and adults (Barth et al., 2023; Heuvel and Sporns, 2019; Kelly et al., 2018).

The increased morphometric similarity observed in the somatomotor network poses a complex challenge for explanation, considering the general neglect of the somatomotor network within psychiatric models of schizophrenia. Speculatively, it may be that increased morphometric similarity for the somatomotor network may be compensatory as individuals with schizophrenia may be less able to draw on other networks. Nonetheless, a recent resting-state fMRI study shed light on altered somatomotor network connectivity, suggesting its potential relevance across various psychiatric disorders, associating it with psychopathology, cognitive impairment, and impulsivity (Kebets et al., 2019).

In a minority of individuals with schizophrenia, infra-normal and supra-normal deviations of morphometric similarity were present (<6%), mirroring observations akin to those found in healthy individuals. Notably, outlier percentages did not differ significantly between baseline and follow-up assessments. These results indicate that variations in morphometric similarity among individuals with schizophrenia

predominantly existed within the spectrum of variations observed in the healthy reference sample (Bedford et al., 2023; ENIGMA Clinical High Risk for Psychosis Working Group et al., 2024; Segal et al., 2023; Winter et al., 2022; Wolfers et al., 2018). Previous normative modeling studies conducted on individuals with schizophrenia or those at high risk for the condition have reported similar percentages for cortical volume and cortical thickness (ENIGMA Clinical High Risk for Psychosis Working Group et al., 2024; Segal et al., 2023; Wolfers et al., 2018). We demonstrated significant heterogeneity in morphometric similarity among individuals with schizophrenia, suggesting that structural deficits in schizophrenia are nuanced and intricate, which contributes to a substantial overlap between individuals with chronic schizophrenia and healthy controls.

The change in total outlier count over time did not differ between cases and controls, meaning that individuals with schizophrenia did not have an accelerated accumulation of outlier regions as compared to the healthy individuals during follow-up. In individuals with Alzheimer's disease, the total outlier count for cortical thickness was increased at baseline and also progressed over time when compared to healthy individuals implying that the outlier count can be used to track neurodegeneration in Alzheimer's disease (Verdi et al., 2023). While morphometric similarity is being increasingly used to detect macroscopic brain abnormalities in individuals with psychiatric disorders, with both regional increases and decreases reported, there is no prior information available about changes of morphometric similarity over time (Li et al., 2021; Morgan et al., 2019). In addition to the change in outlier count we showed that the increase and decrease of the regional outlier percentage during follow-up was relatively small and similar in both cases and controls (<|4|%). This indicates that of those with baseline regional morphometric

similarity values outside the normative range few fluctuated considerably over time. For schizophrenia it may mean that change in regional cortical thickness over time, as assessed by normative modeling, is more sensitive to disease effects compared to regional morphometric similarity (Barbora Rehák Bučková et al., 2024). Taken together, our results could imply that morphometric similarity may have restricted utility in elucidating the pathophysiology of schizophrenia (Winter et al., 2022).

Normative models may be better able to detect diagnosis-related effects compared to raw, i.e. traditional, data models because normative modeling allows for the consideration of numerous sources of variance. Some of these sources may not carry clinical significance (e.g., scanner variability, Euler number), while others simultaneously encapsulate clinically relevant information within the framework of a reference cohort. Our supplemental results are in line with this, i.e. our study demonstrated increased statistical significance using normative models when compared to raw data models. Thus, normative modeling may possess the capacity to capture overarching population patterns, discern clinical disparities between groups, and retain the ability to investigate individual differences (Rutherford et al., 2023).

This study has limitations. For clinical translation, progressions in normative modeling stand as a crucial prerequisite, underscoring the necessity for a broadened diversification of datasets. While the present study benefited from a substantial training set, larger and more heterogeneous datasets, incorporating not solely European ancestry data, are imperative for heightened performance and validity (Bethlehem et al., 2022). The normative modeling framework employed herein treats each region as independent, notwithstanding potential correlations among z-scores from neighboring regions. To mitigate this challenge, one plausible strategy involves

implementing data reduction techniques, such as principal component analysis applied to the z-scores (Rutherford et al., 2022). While our sample size of individuals with schizophrenia was comparable to previous normative modeling studies, larger (multicenter) clinical samples may enable the identification of distinct clusters of patients exhibiting significant deviance (Rutherford et al., 2023; Wolfers et al., 2018).

In conclusion, the current study used normative modeling to show decreased morphometric similarity of the default mode network in a group of individuals with chronic schizophrenia, replicating previous findings in groups of individuals with first-episode psychosis. Using a longitudinal design we showed that the change in total number of outlier regions over time was not different between cases and controls. Change over time of the regional percentage of outliers was low indicating only few participants showed large changes over time. Normative modeling demonstrated that significant cross-sectional reductions and longitudinal changes of morphometric similarity are only present in a minority of individuals with schizophrenia. Our study provides a lay out for future studies using normative modeling including cross-sectional and longitudinal neuroimaging phenotypes.

References

Alnæs D, Kaufmann T, van der Meer D, Córdova-Palomera A, Rokicki J, Moberget T, Bettella F, Agartz I, Barch DM, Bertolino A, Brandt CL, Cervenka S, Djurovic S, Doan NT, Eisenacher S, Fatouros-Bergman H, Flyckt L, Di Giorgio A, Haatveit B, Jönsson EG, Kirsch P, Lund MJ, Meyer-Lindenberg A, Pergola G, Schwarz E, Smeland OB, Quarto T, Zink M, Andreassen OA, Westlye LT, Karolinska Schizophrenia Project Consortium. 2019. Brain Heterogeneity in Schizophrenia and Its Association With Polygenic Risk. *JAMA Psychiatry* **76**:739–748. doi:10.1001/jamapsychiatry.2019.0257

Barbora Rehák Bučková, Charlotte Fraza, Rastislav Rehák, Marián Kolenič, Christian Beckmann, Filip Španiel, Andre Marquand, Jaroslav Hlinka. 2024. Using normative models pre-trained on cross-sectional data to evaluate longitudinal changes in neuroimaging data. *bioRxiv* 2023.06.09.544217. doi:10.1101/2023.06.09.544217

Barth C, Kelly S, Nerland S, Jahanshad N, Alloza C, Ambrogi S, Andreassen OA, Andreou D, Arango C, Baeza I, Banaj N, Bearden CE, Berk M, Bohman H, Castro-Fornieles J, Chye Y, Crespo-Facorro B, de la Serna E, Díaz-Caneja CM, Gurholt TP, Hegarty CE, James A, Janssen J, Johannessen C, Jönsson EG, Karlsgodt KH, Kochunov P, Lois NG, Lundberg M, Myhre AM, Pascual-Diaz S, Piras F, Smelror RE, Spalletta G, Stokkan TS, Sugranyes G, Suo C, Thomopoulos SI, Tordesillas-Gutiérrez D, Vecchio D, Wedervang-Resell K, Wortinger LA, Thompson PM, Agartz I. 2023. In vivo white matter microstructure in adolescents with early-onset psychosis: a multi-site mega-analysis. *Mol Psychiatry* **28**:1159–1169. doi:10.1038/s41380-022-01901-3

Bedford SA, Lai M-C, Lombardo MV, Chakrabarti B, Ruigrok A, Suckling J, Anagnostou E, Lerch JP, Taylor M, Nicolson R, Stelios G, Crosbie J, Schachar R, Kelley E, Jones J, Arnold PD, Courchesne E, Pierce K, Eyler LT, Campbell K, Barnes CC, Seidlitz J, Alexander-Bloch AF, Bullmore ET, Baron-Cohen S, Bethlehem RAI, MRC AIMS Consortium and Lifespan Brain Chart Consortium. 2023. Brain-charting autism and attention deficit hyperactivity disorder reveals distinct and overlapping neurobiology. *MedRxiv Prepr Serv Health Sci* 2023.12.06.23299587. doi:10.1101/2023.12.06.23299587

Bethlehem R a. I, Seidlitz J, White SR, Vogel JW, Anderson KM, Adamson C, Adler S, Alexopoulos GS, Anagnostou E, Areces-Gonzalez A, Astle DE, Auyeung B, Ayub M, Bae J, Ball G, Baron-Cohen S, Beare R, Bedford SA, Benegal V, Beyer F, Blangero J, Blesa Cábez M, Boardman JP, Borzage M, Bosch-Bayard JF, Bourke N, Calhoun VD, Chakravarty MM, Chen C, Chertavian C, Chetelat G, Chong YS, Cole JH, Corvin A, Costantino M, Courchesne E, Crivello F, Cropley VL, Crosbie J, Crossley N, Delarue M, Delorme R, Desrivieres S, Devenyi GA, Di Biase MA, Dolan R, Donald KA, Donohoe G, Dunlop K, Edwards AD, Elison JT, Ellis CT, Elman JA, Eyler L, Fair DA, Feczko E, Fletcher PC, Fonagy P, Franz CE, Galan-Garcia L, Gholipour A, Giedd J, Gilmore JH, Glahn DC, Goodyer IM, Grant PE, Groenewold NA, Gunning FM, Gur RE, Gur RC, Hammill CF, Hansson O, Hedden T, Heinz A, Henson RN, Heuer K, Hoare J, Holla B, Holmes AJ, Holt R, Huang H, Im K, Ipser J, Jack CR, Jackowski AP, Jia T, Johnson KA, Jones PB, Jones DT, Kahn RS, Karlsson H, Karlsson L, Kawashima R, Kelley EA, Kern S, Kim KW, Kitzbichler MG, Kremen WS, Lalonde F, Landeau B, Lee S, Lerch J, Lewis JD, Li J, Liao W, Liston C, Lombardo MV, Lv J, Lynch C,

Mallard TT, Marcelis M, Markello RD, Mathias SR, Mazoyer B, McGuire P, Meaney MJ, Mechelli A, Medic N, Misic B, Morgan SE, Mothersill D, Nigg J, Ong MQW, Ortinau C, Ossenkoppele R, Ouyang M, Palaniyappan L, Paly L, Pan PM, Pantelis C, Park MM, Paus T, Pausova Z, Paz-Linares D, Pichet Binette A, Pierce K, Qian X, Qiu J, Qiu A, Raznahan A, Rittman T, Rodrigue A, Rollins CK, Romero-Garcia R, Ronan L, Rosenberg MD, Rowitch DH, Salum GA, Satterthwaite TD, Schaare HL, Schachar RJ, Schultz AP, Schumann G, Schöll M, Sharp D, Shinohara RT, Skoog I, Smyser CD, Sperling RA, Stein DJ, Stolicyn A, Suckling J, Sullivan G, Taki Y, Thyreau B, Toro R, Traut N, Tsvetanov KA, Turk-Browne NB, Tuulari JJ, Tzourio C, Vachon-Presseau É, Valdes-Sosa MJ, Valdes-Sosa PA, Valk SL, van Amelsvoort T, Vandekar SN, Vasung L, Victoria LW, Villeneuve S, Villringer A, Vértes PE, Wagstyl K, Wang YS, Warfield SK, Warrier V, Westman E, Westwater ML, Whalley HC, Witte AV, Yang N, Yeo B, Yun H, Zalesky A, Zar HJ, Zettergren A, Zhou JH, Ziauddeen H, Zugman A, Zuo XN, 3R-BRAIN, AIBL, Alzheimer's Disease Neuroimaging Initiative, Alzheimer's Disease Repository Without Borders Investigators, CALM Team, Cam-CAN, CCNP, COBRE, cVEDA, ENIGMA Developmental Brain Age Working Group, Developing Human Connectome Project, FinnBrain, Harvard Aging Brain Study, IMAGEN, KNE96, Mayo Clinic Study of Aging, NSPN, POND, PREVENT-AD Research Group, VETSA, Bullmore ET, Alexander-Bloch AF. 2022. Brain charts for the human lifespan. *Nature* **604**:525–533. doi:10.1038/s41586-022-04554-y

Bethlehem RAI, Seidlitz J, Romero-Garcia R, Trakoshis S, Dumas G, Lombardo MV. 2020. A normative modelling approach reveals age-atypical cortical thickness

in a subgroup of males with autism spectrum disorder. *Commun Biol* **3**:486. doi:10.1038/s42003-020-01212-9

Broyd SJ, Demanuele C, Debener S, Helps SK, James CJ, Sonuga-Barke EJS. 2009. Default-mode brain dysfunction in mental disorders: a systematic review. *Neurosci Biobehav Rev* **33**:279–296. doi:10.1016/j.neubiorev.2008.09.002

Brugger SP, Howes OD. 2017. Heterogeneity and Homogeneity of Regional Brain Structure in Schizophrenia: A Meta-analysis. *JAMA Psychiatry* **74**:1104–1111. doi:10.1001/jamapsychiatry.2017.2663

Charrad M, Ghazzali N, Boiteau V, Niknafs A. 2014. NbClust: An R Package for Determining the Relevant Number of Clusters in a Data Set. *J Stat Softw* **61**:1–36. doi:10.18637/jss.v061.i06

Cox SR, Ritchie SJ, Tucker-Drob EM, Liewald DC, Hagenaars SP, Davies G, Wardlaw JM, Gale CR, Bastin ME, Deary IJ. 2016. Ageing and brain white matter structure in 3,513 UK Biobank participants. *Nat Commun* **7**:13629. doi:10.1038/ncomms13629

Di Biase MA, Geaghan MP, Reay WR, Seidlitz J, Weickert CS, Pébay A, Green MJ, Quidé Y, Atkins JR, Coleman MJ, Bouix S, Knyazhanskaya EE, Lyall AE, Pasternak O, Kubicki M, Rathi Y, Visco A, Gaunnac M, Lv J, Mesholam-Gately RI, Lewandowski KE, Holt DJ, Keshavan MS, Pantelis C, Öngür D, Breier A, Cairns MJ, Shenton ME, Zalesky A. 2022. Cell type-specific manifestations of cortical thickness heterogeneity in schizophrenia. *Mol Psychiatry* **27**:2052–2060. doi:10.1038/s41380-022-01460-7

Di Biase MA, Tian YE, Bethlehem RAI, Seidlitz J, Alexander-Bloch AF, Yeo BTT, Zalesky A. 2023. Mapping human brain charts cross-sectionally and

longitudinally. *Proc Natl Acad Sci U S A* **120**:e2216798120.

doi:10.1073/pnas.2216798120

ENIGMA Clinical High Risk for Psychosis Working Group, Haas SS, Ge R, Agartz I, Amminger GP, Andreassen OA, Bachman P, Baeza I, Choi S, Colibazzi T, Cropley VL, de la Fuente-Sandoval C, Ebdrup BH, Fortea A, Fusar-Poli P, Glenthøj BY, Glenthøj LB, Haut KM, Hayes RA, Heekeren K, Hooker CI, Hwang WJ, Jahanshad N, Kaess M, Kasai K, Katagiri N, Kim M, Kindler J, Koike S, Kristensen TD, Kwon JS, Lawrie SM, Lebedeva I, Lee J, Lemmers-Jansen ILJ, Lin A, Ma X, Mathalon DH, McGuire P, Michel C, Mizrahi R, Mizuno M, Møller P, Mora-Durán R, Nelson B, Nemoto T, Nordentoft M, Nordholm D, Omelchenko MA, Pantelis C, Pariente JC, Raghava JM, Reyes-Madrigal F, Røssberg JI, Rössler W, Salisbury DF, Sasabayashi D, Schall U, Smigielski L, Sugranyes G, Suzuki M, Takahashi T, Tamnes CK, Theodoridou A, Thomopoulos SI, Thompson PM, Tomyshev AS, Uhlhaas PJ, Værnes TG, van Amelsvoort TAMJ, van Erp TGM, Waltz JA, Wenneberg C, Westlye LT, Wood SJ, Zhou JH, Hernaus D, Jalbrzikowski M, Kahn RS, Corcoran CM, Frangou S. 2024. Normative Modeling of Brain Morphometry in Clinical High Risk for Psychosis. *JAMA Psychiatry* **81**:77–88.

doi:10.1001/jamapsychiatry.2023.3850

Fischl B. 2012. FreeSurfer. *NeuroImage* **62**:774–781.

doi:10.1016/j.neuroimage.2012.01.021

Fraza CJ, Dinga R, Beckmann CF, Marquand AF. 2021. Warped Bayesian linear regression for normative modelling of big data. *NeuroImage* **245**:118715.

doi:10.1016/j.neuroimage.2021.118715

Geerligs L, Renken RJ, Saliasi E, Maurits NM, Lorist MM. 2015. A Brain-Wide Study

of Age-Related Changes in Functional Connectivity. *Cereb Cortex N Y N 1991* **25**:1987–1999. doi:10.1093/cercor/bhu012

Haijma SV, Van Haren N, Cahn W, Koolschijn PCMP, Hulshoff Pol HE, Kahn RS. 2013. Brain volumes in schizophrenia: a meta-analysis in over 18 000 subjects. *Schizophr Bull* **39**:1129–1138. doi:10.1093/schbul/sbs118

Heuvel MP van den, Sporns O. 2019. A cross-disorder connectome landscape of brain dysconnectivity. *Nat Rev Neurosci* **20**:435. doi:10.1038/s41583-019-0177-6

Huang AS, Kang K, Vandekar S, Rogers BP, Heckers S, Woodward ND. 2024. Lifespan development of thalamic nuclei and characterizing thalamic nuclei abnormalities in schizophrenia using normative modeling. *Neuropsychopharmacol Off Publ Am Coll Neuropsychopharmacol*. doi:10.1038/s41386-024-01837-y

Hulshoff Pol HE, Schnack HG, Mandl RC, van Haren NE, Koning H, Collins DL, Evans AC, Kahn RS. 2001. Focal gray matter density changes in schizophrenia. *Arch Gen Psychiatry* **58**:1118–1125. doi:10.1001/archpsyc.58.12.1118

Janssen J, Díaz-Caneja CM, Alloza C, Schippers A, de Hoyos L, Santonja J, Gordaliza PM, Buimer EEL, van Haren NEM, Cahn W, Arango C, Kahn RS, Hulshoff Pol HE, Schnack HG. 2021. Dissimilarity in Sulcal Width Patterns in the Cortex can be Used to Identify Patients With Schizophrenia With Extreme Deficits in Cognitive Performance. *Schizophr Bull* **47**:552–561. doi:10.1093/schbul/sbaa131

Jauhar S, Johnstone M, McKenna PJ. 2022. Schizophrenia. *Lancet Lond Engl* **399**:473–486. doi:10.1016/S0140-6736(21)01730-X

Kay SR, Fiszbein A, Opler LA. 1987. The positive and negative syndrome scale (PANSS) for schizophrenia. *Schizophr Bull* **13**:261–276. doi:10.1093/schbul/13.2.261

Kebets V, Holmes AJ, Orban C, Tang S, Li J, Sun N, Kong R, Poldrack RA, Yeo BTT. 2019. Somatosensory-Motor Dysconnectivity Spans Multiple Transdiagnostic Dimensions of Psychopathology. *Biol Psychiatry* **86**:779–791. doi:10.1016/j.biopsych.2019.06.013

Kelly S, Jahanshad N, Zalesky A, Kochunov P, Agartz I, Alloza C, Andreassen OA, Arango C, Banaj N, Bouix S, Bousman CA, Brouwer RM, Bruggemann J, Bustillo J, Cahn W, Calhoun V, Cannon D, Carr V, Catts S, Chen J, Chen J-X, Chen X, Chiapponi C, Cho KK, Ciullo V, Corvin AS, Crespo-Facorro B, Cropley V, De Rossi P, Diaz-Caneja CM, Dickie EW, Ehrlich S, Fan F-M, Faskowitz J, Fatouros-Bergman H, Flyckt L, Ford JM, Fouche J-P, Fukunaga M, Gill M, Glahn DC, Gollub R, Goudzwaard ED, Guo H, Gur RE, Gur RC, Gurholt TP, Hashimoto R, Hatton SN, Henskens FA, Hibar DP, Hickie IB, Hong LE, Horacek J, Howells FM, Hulshoff Pol HE, Hyde CL, Isaev D, Jablensky A, Jansen PR, Janssen J, Jönsson EG, Jung LA, Kahn RS, Kikinis Z, Liu K, Klauser P, Knöchel C, Kubicki M, Lagopoulos J, Langen C, Lawrie S, Lenroot RK, Lim KO, Lopez-Jaramillo C, Lyall A, Magnotta V, Mandl RCW, Mathalon DH, McCarley RW, McCarthy-Jones S, McDonald C, McEwen S, McIntosh A, Melicher T, Mesholam-Gately RI, Michie PT, Mowry B, Mueller BA, Newell DT, O'Donnell P, Oertel-Knöchel V, Oestreich L, Paciga SA, Pantelis C, Pasternak O, Pearlson G, Pellicano GR, Pereira A, Pineda Zapata J, Piras F, Potkin SG, Preda A, Rasser PE, Roalf DR, Roiz R, Roos A, Rotenberg D, Satterthwaite TD, Savadjiev P, Schall U, Scott RJ, Seal ML,

Seidman LJ, Shannon Weickert C, Whelan CD, Shenton ME, Kwon JS, Spalletta G, Spaniel F, Sprooten E, Stäblein M, Stein DJ, Sundram S, Tan Y, Tan S, Tang S, Temmingh HS, Westlye LT, Tønnesen S, Tordesillas-Gutierrez D, Doan NT, Vaidya J, van Haren NEM, Vargas CD, Vecchio D, Velakoulis D, Voineskos A, Voyvodic JQ, Wang Z, Wan P, Wei D, Weickert TW, Whalley H, White T, Whitford TJ, Wojcik JD, Xiang H, Xie Z, Yamamori H, Yang F, Yao N, Zhang G, Zhao J, van Erp TGM, Turner J, Thompson PM, Donohoe G. 2018. Widespread white matter microstructural differences in schizophrenia across 4322 individuals: results from the ENIGMA Schizophrenia DTI Working Group. *Mol Psychiatry* **23**:1261–1269. doi:10.1038/mp.2017.170

Klein A, Tourville J. 2012. 101 labeled brain images and a consistent human cortical labeling protocol. *Front Neurosci* **6**:171. doi:10.3389/fnins.2012.00171

Korver N, Quee PJ, Boos HBM, Simons CJP, de Haan L, GROUP investigators. 2012. Genetic Risk and Outcome of Psychosis (GROUP), a multi-site longitudinal cohort study focused on gene-environment interaction: objectives, sample characteristics, recruitment and assessment methods. *Int J Methods Psychiatr Res* **21**:205–221. doi:10.1002/mpr.1352

Kubota M, van Haren NEM, Haijma SV, Schnack HG, Cahn W, Hulshoff Pol HE, Kahn RS. 2015. Association of IQ Changes and Progressive Brain Changes in Patients With Schizophrenia. *JAMA Psychiatry* **72**:803–812. doi:10.1001/jamapsychiatry.2015.0712

Li J, Seidlitz J, Suckling J, Fan F, Ji G-J, Meng Y, Yang S, Wang K, Qiu J, Chen H, Liao W. 2021. Cortical structural differences in major depressive disorder correlate with cell type-specific transcriptional signatures. *Nat Commun* **12**:1647. doi:10.1038/s41467-021-21943-5

Lin S, Lv X, Lin X, Chen S, Li Y, Xu M, Qiu Y, Tang L. 2024. Modulation Effects of the CEP128 Gene on Radiotherapy-Related Brain Injury: A Longitudinal Structural Study Using Multi-Parametric Brain MR Images. *J Magn Reson Imaging JMRI* **59**:648–658. doi:10.1002/jmri.28824

Lu H, Xu F, Rodrigue KM, Kennedy KM, Cheng Y, Flicker B, Hebrank AC, Uh J, Park DC. 2011. Alterations in cerebral metabolic rate and blood supply across the adult lifespan. *Cereb Cortex N Y N 1991* **21**:1426–1434. doi:10.1093/cercor/bhq224

Lv J, Di Biase M, Cash RFH, Cocchi L, Cropley VL, Klauser P, Tian Y, Bayer J, Schmaal L, Cetin-Karayumak S, Rathi Y, Pasternak O, Bousman C, Pantelis C, Calamante F, Zalesky A. 2021. Individual deviations from normative models of brain structure in a large cross-sectional schizophrenia cohort. *Mol Psychiatry* **26**:3512–3523. doi:10.1038/s41380-020-00882-5

Marcus DS, Fotenos AF, Csernansky JG, Morris JC, Buckner RL. 2010. Open access series of imaging studies: longitudinal MRI data in nondemented and demented older adults. *J Cogn Neurosci* **22**:2677–2684. doi:10.1162/jocn.2009.21407

Marquand AF, Kia SM, Zabihi M, Wolfers T, Buitelaar JK, Beckmann CF. 2019. Conceptualizing mental disorders as deviations from normative functioning. *Mol Psychiatry* **24**:1415–1424. doi:10.1038/s41380-019-0441-1

Morgan SE, Seidlitz J, Whitaker KJ, Romero-Garcia R, Clifton NE, Scarpazza C, van Amelsvoort T, Marcelis M, van Os J, Donohoe G, Mothersill D, Corvin A, Pocklington A, Raznahan A, McGuire P, Vértes PE, Bullmore ET. 2019. Cortical patterning of abnormal morphometric similarity in psychosis is associated with brain expression of schizophrenia-related genes. *Proc Natl*

Acad Sci U S A **116**:9604–9609. doi:10.1073/pnas.1820754116

Nastase SA, Liu Y-F, Hillman H, Zadbood A, Hasenfratz L, Keshavarzian N, Chen J, Honey CJ, Yeshurun Y, Regev M, Nguyen M, Chang CHC, Baldassano C, Lositsky O, Simony E, Chow MA, Leong YC, Brooks PP, Micciche E, Choe G, Goldstein A, Vanderwal T, Halchenko YO, Norman KA, Hasson U. 2021. The "Narratives" fMRI dataset for evaluating models of naturalistic language comprehension. *Sci Data* **8**:250. doi:10.1038/s41597-021-01033-3

Nooner KB, Colcombe SJ, Tobe RH, Mennes M, Benedict MM, Moreno AL, Panek LJ, Brown S, Zavitz ST, Li Q, Sikka S, Gutman D, Bangaru S, Schlachter RT, Kamiel SM, Anwar AR, Hinz CM, Kaplan MS, Rachlin AB, Adelsberg S, Cheung B, Khanuja R, Yan C, Craddock CC, Calhoun V, Courtney W, King M, Wood D, Cox CL, Kelly AMC, Di Martino A, Petkova E, Reiss PT, Duan N, Thomsen D, Biswal B, Coffey B, Hoptman MJ, Javitt DC, Pomara N, Sidtis JJ, Koplewicz HS, Castellanos FX, Leventhal BL, Milham MP. 2012. The NKI-Rockland Sample: A Model for Accelerating the Pace of Discovery Science in Psychiatry. *Front Neurosci* **6**:152. doi:10.3389/fnins.2012.00152

Pang JC, Aquino KM, Oldehinkel M, Robinson PA, Fulcher BD, Breakspear M, Fornito A. 2023. Geometric constraints on human brain function. *Nature* **618**:566–574. doi:10.1038/s41586-023-06098-1

Rosen AFG, Roalf DR, Ruparel K, Blake J, Seelaus K, Villa LP, Ciric R, Cook PA, Davatzikos C, Elliott MA, Garcia de La Garza A, Gennatas ED, Quarmley M, Schmitt JE, Shinohara RT, Tisdall MD, Craddock RC, Gur RE, Gur RC, Satterthwaite TD. 2018. Quantitative assessment of structural image quality. *NeuroImage* **169**:407–418. doi:10.1016/j.neuroimage.2017.12.059

Rutherford S, Barkema P, Tso IF, Sripada C, Beckmann CF, Ruhe HG, Marquand AF.

2023. Evidence for embracing normative modeling. *eLife* **12**:e85082. doi:10.7554/eLife.85082

Rutherford S, Kia SM, Wolfers T, Fraza C, Zabihi M, Dinga R, Berthet P, Worker A, Verdi S, Ruhe HG, Beckmann CF, Marquand AF. 2022. The normative modeling framework for computational psychiatry. *Nat Protoc* **17**:1711–1734. doi:10.1038/s41596-022-00696-5

Sebenius I, Seidlitz J, Warrier V, Bethlehem RAI, Alexander-Bloch A, Mallard TT, Garcia RR, Bullmore ET, Morgan SE. 2023. Robust estimation of cortical similarity networks from brain MRI. *Nat Neurosci* **26**:1461–1471. doi:10.1038/s41593-023-01376-7

Segal A, Parkes L, Aquino K, Kia SM, Wolfers T, Franke B, Hoogman M, Beckmann CF, Westlye LT, Andreassen OA, Zalesky A, Harrison BJ, Davey CG, Soriano-Mas C, Cardoner N, Tiego J, Yücel M, Braganza L, Suo C, Berk M, Cotton S, Bellgrove MA, Marquand AF, Fornito A. 2023. Regional, circuit and network heterogeneity of brain abnormalities in psychiatric disorders. *Nat Neurosci* **26**:1613–1629. doi:10.1038/s41593-023-01404-6

Seidlitz J, Váša F, Shinn M, Romero-Garcia R, Whitaker KJ, Vértes PE, Wagstyl K, Kirkpatrick Reardon P, Clasen L, Liu S, Messinger A, Leopold DA, Fonagy P, Dolan RJ, Jones PB, Goodyer IM, NSPN Consortium, Raznahan A, Bullmore ET. 2018. Morphometric Similarity Networks Detect Microscale Cortical Organization and Predict Inter-Individual Cognitive Variation. *Neuron* **97**:231-247.e7. doi:10.1016/j.neuron.2017.11.039

Shafto MA, Tyler LK, Dixon M, Taylor JR, Rowe JB, Cusack R, Calder AJ, Marslen-Wilson WD, Duncan J, Dalgleish T, Henson RN, Brayne C, Matthews FE, Cam-CAN. 2014. The Cambridge Centre for Ageing and Neuroscience

(Cam-CAN) study protocol: a cross-sectional, lifespan, multidisciplinary examination of healthy cognitive ageing. *BMC Neurol* **14**:204. doi:10.1186/s12883-014-0204-1

Snoek L, van der Miesen MM, Beemsterboer T, van der Leij A, Eigenhuis A, Steven Scholte H. 2021. The Amsterdam Open MRI Collection, a set of multimodal MRI datasets for individual difference analyses. *Sci Data* **8**:85. doi:10.1038/s41597-021-00870-6

Thomas Yeo BT, Krienen FM, Sepulcre J, Sabuncu MR, Lashkari D, Hollinshead M, Roffman JL, Smoller JW, Zöllei L, Polimeni JR, Fischl B, Liu H, Buckner RL. 2011. The organization of the human cerebral cortex estimated by intrinsic functional connectivity. *J Neurophysiol* **106**:1125–1165. doi:10.1152/jn.00338.2011

van Erp TGM, Walton E, Hibar DP, Schmaal L, Jiang W, Glahn DC, Pearlson GD, Yao N, Fukunaga M, Hashimoto R, Okada N, Yamamori H, Bustillo JR, Clark VP, Agartz I, Mueller BA, Cahn W, de Zwarte SMC, Hulshoff Pol HE, Kahn RS, Ophoff RA, van Haren NEM, Andreassen OA, Dale AM, Doan NT, Gurholt TP, Hartberg CB, Haukvik UK, Jørgensen KN, Lagerberg TV, Melle I, Westlye LT, Gruber O, Kraemer B, Richter A, Zilles D, Calhoun VD, Crespo-Facorro B, Roiz-Santiañez R, Tordesillas-Gutiérrez D, Loughland C, Carr VJ, Catts S, Cropley VL, Fullerton JM, Green MJ, Henskens FA, Jablensky A, Lenroot RK, Mowry BJ, Michie PT, Pantelis C, Quidé Y, Schall U, Scott RJ, Cairns MJ, Seal M, Tooney PA, Rasser PE, Cooper G, Shannon Weickert C, Weickert TW, Morris DW, Hong E, Kochunov P, Beard LM, Gur RE, Gur RC, Satterthwaite TD, Wolf DH, Belger A, Brown GG, Ford JM, Macciardi F, Mathalon DH, O'Leary DS, Potkin SG, Preda A, Voyvodic J, Lim KO, McEwen

S, Yang F, Tan Y, Tan S, Wang Z, Fan F, Chen J, Xiang H, Tang S, Guo H, Wan P, Wei D, Bockholt HJ, Ehrlich S, Wolthusen RPF, King MD, Shoemaker JM, Sponheim SR, De Haan L, Koenders L, Machielsen MW, van Amelsvoort T, Veltman DJ, Assogna F, Banaj N, de Rossi P, Iorio M, Piras F, Spalletta G, McKenna PJ, Pomarol-Clotet E, Salvador R, Corvin A, Donohoe G, Kelly S, Whelan CD, Dickie EW, Rotenberg D, Voineskos AN, Ciufolini S, Radua J, Dazzan P, Murray R, Reis Marques T, Simmons A, Borgwardt S, Egloff L, Harrisberger F, Riecher-Rössler A, Smieskova R, Alpert KI, Wang L, Jönsson EG, Koops S, Sommer IEC, Bertolino A, Bonvino A, Di Giorgio A, Neilson E, Mayer AR, Stephen JM, Kwon JS, Yun J-Y, Cannon DM, McDonald C, Lebedeva I, Tomyshev AS, Akhadov T, Kaleda V, Fatouros-Bergman H, Flyckt L, Karolinska Schizophrenia Project, Busatto GF, Rosa PGP, Serpa MH, Zanetti MV, Hoschl C, Skoch A, Spaniel F, Tomecek D, Hagenaars SP, McIntosh AM, Whalley HC, Lawrie SM, Knöchel C, Oertel-Knöchel V, Stäblein M, Howells FM, Stein DJ, Temmingh HS, Uhlmann A, Lopez-Jaramillo C, Dima D, McMahon A, Faskowitz JI, Gutman BA, Jahanshad N, Thompson PM, Turner JA. 2018. Cortical Brain Abnormalities in 4474 Individuals With Schizophrenia and 5098 Control Subjects via the Enhancing Neuro Imaging Genetics Through Meta Analysis (ENIGMA) Consortium. *Biol Psychiatry* **84**:644–654. doi:10.1016/j.biopsych.2018.04.023

Váša F, Seidlitz J, Romero-Garcia R, Whitaker KJ, Rosenthal G, Vértes PE, Shinn M, Alexander-Bloch A, Fonagy P, Dolan RJ, Jones PB, Goodyer IM, NSPN consortium, Sporns O, Bullmore ET. 2018. Adolescent Tuning of Association Cortex in Human Structural Brain Networks. *Cereb Cortex N Y N 1991* **28**:281–294. doi:10.1093/cercor/bhx249

Verdi S, Rutherford S, Fraza C, Tosun D, Altmann A, Raket LL, Schott JM, Marquand AF, Cole JH, Alzheimer's Disease Neuroimaging Initiative. 2023. Personalising Alzheimer's Disease progression using brain atrophy markers. *MedRxiv Prepr Serv Health Sci* 2023.06.15.23291418. doi:10.1101/2023.06.15.23291418

Wei D, Zhuang K, Ai L, Chen Q, Yang W, Liu W, Wang K, Sun J, Qiu J. 2018. Structural and functional brain scans from the cross-sectional Southwest University adult lifespan dataset. *Sci Data* **5**:180134. doi:10.1038/sdata.2018.134

Whitfield-Gabrieli S, Thermenos HW, Milanovic S, Tsuang MT, Faraone SV, McCarley RW, Shenton ME, Green AI, Nieto-Castanon A, LaViolette P, Wojcik J, Gabrieli JDE, Seidman LJ. 2009. Hyperactivity and hyperconnectivity of the default network in schizophrenia and in first-degree relatives of persons with schizophrenia. *Proc Natl Acad Sci U S A* **106**:1279–1284. doi:10.1073/pnas.0809141106

Winter NR, Leenings R, Ernsting J, Sarink K, Fisch L, Emden D, Blanke J, Goltermann J, Opel N, Barkhau C, Meinert S, Dohm K, Repple J, Mauritz M, Gruber M, Leehr EJ, Grotegerd D, Redlich R, Jansen A, Nenadic I, Nöthen MM, Forstner A, Rietschel M, Groß J, Bauer J, Heindel W, Andlauer T, Eickhoff SB, Kircher T, Dannlowski U, Hahn T. 2022. Quantifying Deviations of Brain Structure and Function in Major Depressive Disorder Across Neuroimaging Modalities. *JAMA Psychiatry* **79**:879–888. doi:10.1001/jamapsychiatry.2022.1780

Wolfers T, Doan NT, Kaufmann T, Alnæs D, Moberget T, Agartz I, Buitelaar JK, Ueland T, Melle I, Franke B, Andreassen OA, Beckmann CF, Westlye LT,

Marquand AF. 2018. Mapping the Heterogeneous Phenotype of

Schizophrenia and Bipolar Disorder Using Normative Models. *JAMA*

Psychiatry **75**:1146–1155. doi:10.1001/jamapsychiatry.2018.2467

Yao G, Zou T, Luo J, Hu S, Yang L, Li J, Li X, Zhang Y, Feng K, Xu Y, Liu P. 2023.

Cortical structural changes of morphometric similarity network in early-onset

schizophrenia correlate with specific transcriptional expression patterns. *BMC*

Med **21**:479. doi:10.1186/s12916-023-03201-1

Zhukovsky P, Savulich G, Morgan S, Dalley JW, Williams GB, Ersche KD. 2022.

Morphometric similarity deviations in stimulant use disorder point towards

abnormal brain ageing. *Brain Commun* **4**:fcac079.

doi:10.1093/braincomms/fcac079

Data availability

The study IDs of the included participants from the ten publicly available datasets, the five regional metrics and regional morphometric similarity from the ten publicly available datasets, the overlap between the DKT atlas and the 7 functional networks, the normative model plots with percentile curves, the Q-Q plots, the information and usage instructions about the docker we created for normative modeling are all available at https://github.com/iamjoostjanssen/NormModel_MorphoSim_SZ.

Aomic (id1000, piop1 and piop2) is available at https://openneuro.org/datasets/ds003097, https://openneuro.org/datasets/ds002785 and https://openneuro.org/datasets/ds002790, camcan is available at https://camcan-archive.mrc-cbu.cam.ac.uk, dlbs is available at https://fcon_1000.projects.nitrc.org/indi/retro/dlbs, ixi is available at http://brain-development.org/ixidataset, narratives is available at https://openneuro.org/datasets/ds002345, oasis3 is available at www.oasis-brains.org, rockland is available at http://fcon_1000.projects.nitrc.org/indi/enhanced and sald is available at http://fcon_1000.projects.nitrc.org/indi/retro/sald.

Acknowledgements

Disclosures

Dr. Díaz-Caneja has received honoraria from Angelini and Viatris. Dr. Arango has been a consultant to or has received honoraria or grants from Acadia, Angelini, Gedeon Richter, Janssen-Cilag, Lundbeck, Otsuka, Roche, Sage, Servier, Shire, Schering-Plough, Sumitomo Dainippon Pharma, Sunovion, and Takeda. Dr. Cahn has received unrestricted research grants from or served as an independent symposium speaker or consultant for Eli Lilly, Bristol-Myers Squibb, Lundbeck, Sanofi-Aventis, Janssen-Cilag, AstraZeneca, and Schering-Plough. The other authors report no financial relationships with commercial interests.

45